

# Identifying Insar Point Scatterers Corresponding to Water Levels within the Urban **Environment**

Lumban-Gaol, Y. A.; Hanssen, R. F.

DOI

10.1109/IGARSS53475.2024.10641328

**Publication date** 

**Document Version** Final published version

Published in

IGARSS 2024 - 2024 IEEE International Geoscience and Remote Sensing Symposium, Proceedings

Citation (APA)

Lumban-Gaol, Y. A., & Hanssen, R. F. (2024). Identifying Insar Point Scatterers Corresponding to Water Levels within the Urban Environment. In *IGARSS 2024 - 2024 IEEE International Geoscience and Remote Sensing Symposium, Proceedings* (pp. 10668-10472). (International Geoscience and Remote Sensing Symposium (IGARSS)). IEEE. https://doi.org/10.1109/IGARSS53475.2024.10641328

To cite this publication, please use the final published version (if applicable). Please check the document version above.

Copyright

Other than for strictly personal use, it is not permitted to download, forward or distribute the text or part of it, without the consent of the author(s) and/or copyright holder(s), unless the work is under an open content license such as Creative Commons.

Please contact us and provide details if you believe this document breaches copyrights.

We will remove access to the work immediately and investigate your claim.

# Green Open Access added to TU Delft Institutional Repository 'You share, we take care!' - Taverne project

https://www.openaccess.nl/en/you-share-we-take-care

Otherwise as indicated in the copyright section: the publisher is the copyright holder of this work and the author uses the Dutch legislation to make this work public.

# IDENTIFYING INSAR POINT SCATTERERS CORRESPONDING TO WATER LEVELS WITHIN THE URBAN ENVIRONMENT

Y.A. Lumban-Gaol and R.F. Hanssen

Delft University of Technology, Department of Geoscience and Remote Sensing Delft, 2628 CN, The Netherlands

# **ABSTRACT**

The repeat period of SAR data and its side-looking characteristics make InSAR time series analysis useful for water level monitoring applications. The standard approach determines corresponding scatterers by focusing the study area on the multipath radar reflections that include the water level. This paper introduces an alternative approach to identifying such signals using two metrics: cosine similarity and temporal differential coherence. The results show that temporal differential coherence can detect phase variations similar to water level by constantly returning high values even when there is an offset, while cosine similarity yields low scores. Within an urban environment, this approach finds point scatterers corresponding to water level changes in or near water, such as permanent floating objects, bridges, and buildings adjacent to water, where the highest differential coherence value was acquired from a permanent floating restaurant in open water.

*Index Terms*— InSAR, phase similarity, point scatterers, temporal coherence, water levels

# 1. INTRODUCTION

Due to the side-looking characteristics of synthetic aperture radar (SAR) satellites and the interferometric (InSAR) analysis of time series, SAR data can be applied to monitor water level variations over natural areas, such as vegetated wetland areas [1, 2, 3, 4, 5, 6, 7] and lakes [8, 9, 10], as well as rivers under a bridge [11, 12]. The principle is that SAR signals from double- or triple-bounce scattering, which occurs between the horizontal water surface and surrounding objects, lead to coherent scatterers sensitive to potential relative water level changes. In this case, the objects in or near the water cause a significant part of the radar reflection to return into the direction of the sensor instead of reflecting in a specular way. The type of objects varies depending on the area of interest, e.g., vertical wetland vegetation in the case of wetland areas, a combination of natural rocks and irregular topography in small lakes within mountainous regions, or bridges crossing a river.

Two SAR observation properties can be used for this objective. The interferometric phase, constructed from pairs of SAR images [13], can be retrieved from phase observations from double-bounce scatterers that include water level variation. On the other hand, it is possible to estimate water level changes using range changes if the multipath backscatter according to water level change is visible on the image stack, e.g., the case with water under the bridge [11, 12]. In this case, the variability of the estimated water level depends on the SAR image's spatial resolution.

Another approach incorporates the InSAR technique to generate digital elevation models (DEMs) for water level monitoring in dam reservoirs [14, 15]. Subsequently, the waterline boundary is detected, e.g., using SAR edge detection algorithms [14, 16]. Based on the boundaries from different SAR acquisitions, the slope distance between two acquisitions can be computed, and the water level variations can be retrieved.

All methods above rely on a straightforward identification of multipath radar reflections that include the water level. Yet, in an urban environment, this is far from trivial, while the consequences of varying water levels directly affect a large number of people. Here we demonstrate that amidst millions of scatterers in an urban setting it is possible to identify those scatterers that contain valuable information on the level of intra-city water bodies.

# 2. MATERIALS AND METHODS

We use an area of  $\sim 1.5 \times 1.5$  km in the center of Amsterdam, the Netherlands, a dense urban area with many interconnected canals and indirect connections to the North Sea, neighboring polders, and natural rivers. The average elevation of the area of interest varies between 0 and 2 m above mean sea level [17]. The city's water level is monitored and recorded using a level gauge every 10 minutes.

As reference, we use the level gauge data provided by Rijkswaterstaat. Since all canals in the study area have the same water level, we use a single level gauge station, at Surinamekade, located approximately 3.5 km east from the study area.

This work was supported by the Indonesian Endowment Fund for Education (LPDP).

Apart from the level gauge we use SAR observations from Sentinel-1A/B using the interferometric wide swath (IW) mode and a single VV polarization, operating in C-band,  $\lambda = 5.55$  cm, with a repeat period of 12 days. Combining the two satellites shortens this to six days. We use the single look complex (SLC) data—to retrieve both the amplitude and phase—from two different geometries, i.e., descending track 37 and ascending track 88. A total of 154 and 152 acquisitions are available from March 2020 to June 2023 for both descending and ascending, respectively.

#### 2.1. Time Series InSAR Phase

Considering the condition of the study area, a standard processing chain for point scatterers (PS) was used to preprocess all SAR data to obtain InSAR phases as described in [18, 19]. All data in the stack was initially coregistered, and then, a single image was selected randomly as a reference in time. Here, the image on 28 March 2020 was used. Then, all interferometric phases were calculated for all data pairs in the stack. The normalized amplitude dispersion (NAD) was employed to filter out points with high dispersion. Considering water level variations, we use a relatively high threshold of 0.6 to include potential PS related to water. In the end, we have 25,222 and 22,518 points for descending and ascending, respectively.

Subsequently, a subset of points was selected to generate a network to calculate the trend phase parameters. The selection is also based on NAD with a smaller threshold of 0.3, so points with NAD lower than the threshold were considered. The parameters were used for the detrending process, and this corrected phase  $(\varphi_{PS})$  was then considered for further analysis.

# 2.2. Tide Gauge Water Level Processing

Tide gauge stations record water levels every 10 minutes. We subtract all water levels from the raw data using the same master timestamp as the InSAR processing to obtain the relative water level in time. The descending satellite passes the study area at 5:50 UTC while ascending at 17:30 UTC, so we select the data at the same timestamp as the reference. Using the geometry of InSAR data acquisition in the line of sight (LoS), we can convert the water level change in cm unit ( $\Delta h$ ) to radians ( $\varphi_{\rm GT}$ ) using the following equation:

$$\varphi_{\rm GT} = \frac{4\pi\Delta h\cos\theta}{\lambda},\tag{1}$$

where incidence angle  $\theta$  is  ${\sim}41^{\circ}$  (descending) and  ${\sim}30^{\circ}$  (ascending) for this area. Then, using the wrapping operator, mod  $(\varphi_{\rm GT}+\pi,2\pi)-\pi$ , we obtain the relative water level change in the same LoS range as InSAR phase  $(\varphi_{\rm GT_{wr}})$ . We use this wrapped phase as the ground truth to be compared with InSAR phases. Additionally, the remainder of the modulo operator was stored as the ambiguities.

#### 2.3. Detection Approach

Based on the assumption that the InSAR phase corresponds to the relative water level and has a similar phase as the ground truth, a similarity between these two phases can be measured using the cosine similarity

$$C_{\text{PS}_i} = \frac{1}{N} \sum_{n=1}^{N} \cos(\varphi_{\text{GT}_{\text{wr},n}} - \varphi_{\text{PS}_{i,n}}), \tag{2}$$

where N is the number of epochs,  $\varphi_{\mathrm{GT}_{\mathrm{wr},n}}$  is the ground truth phase at n-th epoch, and  $\varphi_{\mathrm{PS}_{i,n}}$  is the InSAR phase of i-th point at n-th epoch. This approach has been used by [20] to identify PS targets between neighboring radar pixels for surface deformation estimation. By computing the cosine of the phase difference, the similarity score C ranges from -1 to 1. A value of 1 represents identical phases, -1 means  $\varphi_{GT}$  and  $\varphi_{PS}$  differ by  $\pi$  rad, while 0 describes that they can be uncorrelated or have an offset of  $\pi/2$ . Since we are interested in retrieving PS having similar phase variations as water level, we argue that the similarity score cannot conclude the corresponding PS due to the possibility of a constant phase offset in the data. Considering this, temporal differential coherence can be used to measure the degree of similarity between two phases by returning high differential coherence, even though the data may have a constant offset. The temporal differential coherence is expressed as [21]

$$\gamma_{\mathrm{PS}_{i}} = \frac{1}{N} \left| \sum_{n=1}^{N} \exp\{j(\varphi_{\mathrm{GT}_{\mathrm{wr},n}} - \varphi_{\mathrm{PS}_{i,n}})\}\right|,\tag{3}$$

Here, we compute both metrics, analyze the results, and select potential PS corresponding to water levels based on one of those measures.

## 3. RESULTS AND DISCUSSION

#### 3.1. PS Corresponding to Water Levels

Using the ground truth water level in the same LoS range as InSAR data, the temporal differential coherence and cosine similarity for the descending track ranges between [0, 0.58] and [-0.51, +0.57] respectively. In Fig. 1a, red PS have high cosine similarity with the ground truth water levels. These are points in or near water associated with objects like houseboats or multipath reflections near bridges. Blue PS are also reflections from those objects and buildings adjacent to canals, leading to a negative cosine similarity. As a comparison, the temporal differential coherence results (see Fig. 1b) show that both the red and the blue PS in Fig. 1a have higher differential coherence than other points. Moreover, the scatter plot in Fig. 1c points out that some PS have low cosine similarity scores but high differential coherence values. Most likely, these experience multipath reflection between water and surrounding objects. On the contrary, PS with high similarity

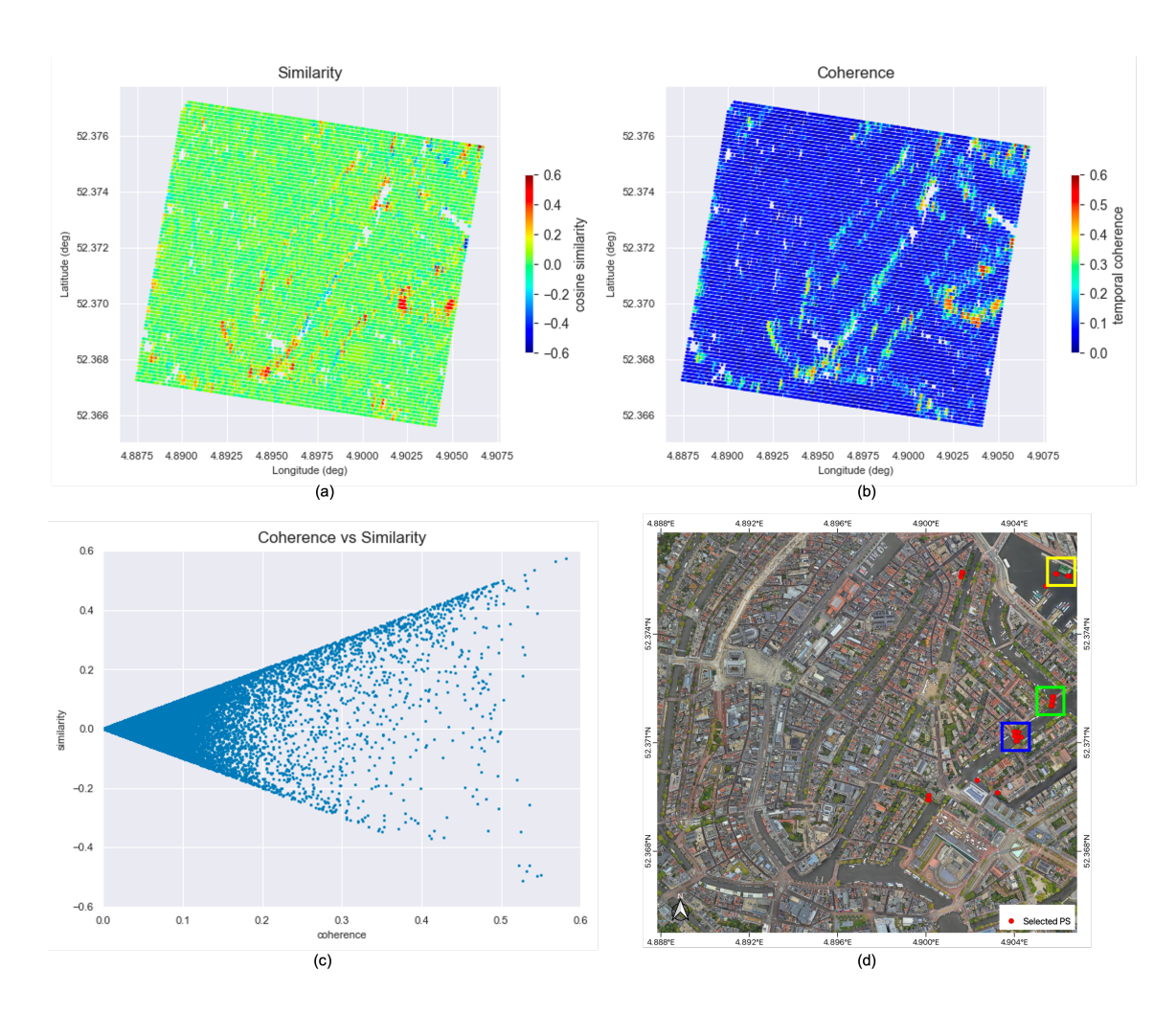


**Fig. 1**. Similarity (a) and differential coherence (b) results of all PS for descending data. The scatter plot (c) represents the distributions of PS against both metrics, which is used to select potential PS associates to water level. The contextual landscape of the study area shows the spatial distribution of selected PS in colored boxes (d). The yellow area represents points close to a floating restaurant in open water. The green box is where scatterers correspond to a tower building, Montelbaanstoren, or a bridge. Similarly, the blue area contains PS associated with a bridge and houseboats.

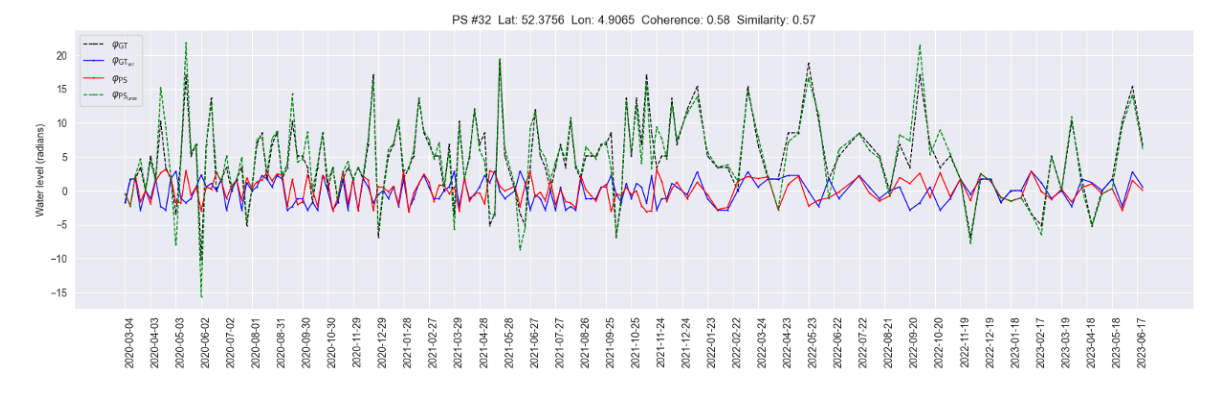


**Fig. 2**. Variability of water levels in radians of the level gauge ground truth, wrapped, in solid blue, and the selected PS, wrapped, in solid red. The dashed lines show the original level gauge data, converted to absolute phase (black-dashed) and the unwrapped PS InSAR phase (green-dashed). Phase unwrapping was performed using the remainder of the modulo operator.

and differential coherence values are presumably correlated to objects directly connected to water level changes, e.g., the houseboats.

These results suggest that the temporal differential coherence is more suitable for identifying potential PS corresponding to water levels than the cosine similarity, since similar water level variability in time can still be detected regardless of an arbitrary constant offset in the data. Accordingly, potential PS selection was performed based on the differential coherence metric. Here, we selected scatterers with a differential coherence greater than 0.5 as potential targets. A total of 30 PS were selected, which can be associated with a bridge or permanent houseboats (blue area), and a bridge or a tower adjacent to water (green area), see Fig. 1d. The highest differential coherence value is obtained from a scatterer associated with a floating restaurant (the yellow area in Fig. 1d). We suspect that the reflection of this PS is directly correlated to water level variations, since the floating restaurant remains at the same spot, causing the observed phases to follow the water levels. Fig. 2 shows how well the InSAR phases of this PS correspond with the level gauge data, where the similarity of one-third of the data is close to 1. Furthermore, after phase unwrapping was performed using the remainder of the modulo operator, the unwrapped water level mainly fits the ground truth.

Based on these results, it is possible to identify PS corresponding to water level changes using temporal differential coherence as a metric to detect scatterers with phase variations similar to water level. However, after PS selection, phase unwrapping is required to retrieve the full phase cycles for water level estimation because the water level variability exceeds the ability of the InSAR fractional phase to observe those changes.

# 3.2. Water Level Variations

Based on a multi-year level gauge observations with a temporal sampling of 10 minutes, water levels vary with a variance of roughly 11 cm. The variability is due to both tidal effects, water run-off variability, and water draining to the sea at ebb tides. As the observed InSAR phase is acquired every six or 12 days, considering one track only we may have several phase cycles of difference between consecutive acquisitions. We could combine several tracks to reduce the revisit period if there is also potential PS corresponding to water levels in other data. However, after processing the ascending data, the temporal differential coherence values appear to be generally much lower than the descending results, with a maximum of  $\sim$ 0.29. Only a few PS can be identified, and these scatterers presumably correspond to houseboats, where some are located in the blue area as in the descending result (Fig. 1d). Considering the geometry of canals, which mainly stretched in a northeast-southwest direction, we hypothesize that the sensor may capture more PS corresponding to water levels when the tre zero-Doppler plane [22] is orthogonal to the canal (descending).

#### 4. CONCLUSIONS AND FURTHER WORKS

We demonstrated two metrics, i.e., cosine similarity and temporal differential coherence, to measure the degree of similarity between two phase series for identifying InSAR PS associated with water levels within an urban area. The results show that temporal differential coherence can detect phase variations similar to water levels even when the phase data has an offset. The potential scatterers can be distinguished into two categories: PS corresponds to objects directly connected to water level changes, and PS with multipath reflection between the water surface and surrounding objects. The highest differential coherence was acquired from the first type of PS, i.e., a permanent floating restaurant in the open water.

After identifying the points, phase unwrapping is required to retrieve the full phase cycles for water level estimation. The accuracy of water level estimation will depend on the accuracy of ambiguity estimation during phase unwrapping. A functional model representing the driving factors of water level variability should be developed to estimate the ambiguity.

## 5. REFERENCES

- [1] Douglas E. Alsdorf, Laurence C. Smith, and John M. Melack, "Amazon floodplain water level changes measured with interferometric SIR-C radar," *IEEE Transactions on Geoscience and Remote Sensing*, vol. 39, no. 2, 2001.
- [2] Shimon Wdowinski, Sang Wan Kim, Falk Amelung, Timothy H. Dixon, Fernando Miralles-Wilhelm, and Roy Sonenshein, "Space-based detection of wetlands' surface water level changes from L-band SAR interferometry," *Remote Sensing of Environment*, vol. 112, no. 3, 2008.
- [3] Jin Woo Kim, Zhong Lu, Hyongki Lee, C. K. Shum, Christopher M. Swarzenski, Thomas W. Doyle, and Sang Ho Baek, "Integrated analysis of PALSAR/Radarsat-1 InSAR and ENVISAT altimeter data for mapping of absolute water level changes in Louisiana wetlands," *Remote Sensing of Environment*, vol. 113, no. 11, 2009.
- [4] Sang Hoon Hong, Shimon Wdowinski, Sang Wan Kim, and Joong Sun Won, "Multi-temporal monitoring of wetland water levels in the Florida Everglades using interferometric synthetic aperture radar (InSAR)," *Remote Sensing of Environment*, vol. 114, no. 11, 2010.

- [5] Meimei Zhang, Zhen Li, Bangsen Tian, Jianmin Zhou, and Panpan Tang, "The backscattering characteristics of wetland vegetation and water-level changes detection using multi-mode SAR: A case study," *International Journal of Applied Earth Observation and Geoinforma*tion, vol. 45, 2016.
- [6] Fernando Jaramillo, Ian Brown, Pascal Castellazzi, Luisa Espinosa, Alice Guittard, Sang Hoon Hong, Victor H. Rivera-Monroy, and Shimon Wdowinski, "Assessment of hydrologic connectivity in an ungauged wetland with InSAR observations," *Environmental Re*search Letters, vol. 13, no. 2, 2018.
- [7] Sebastián Palomino-Ángel, Jesús A. Anaya-Acevedo, Marc Simard, Tien Hao Liao, and Fernando Jaramillo, "Analysis of floodplain dynamics in the Atrato River Colombia using SAR interferometry," Water (Switzer-land), vol. 11, no. 5, 2019.
- [8] D. D. Alexakis, E. G. Stavroulaki, and I. K. Tsanis, "Using Sentinel-1A DInSAR interferometry and Landsat 8 data for monitoring water level changes in two lakes in Crete, Greece," *Geocarto International*, vol. 34, no. 7, 2019.
- [9] S. Palomino-Ángel, R. F. Vázquez, H. Hampel, J. A. Anaya, P. V. Mosquera, S. W. Lyon, and F. Jaramillo, "Retrieval of Simultaneous Water-Level Changes in Small Lakes With InSAR," 2022.
- [10] R. Reyes, M. Nagai, and A. Blanco, "Lake water level variability determination from SAR backscatter of discrete objects, GNSS levelling and satellite altimetry," *Survey Review*, vol. 54, no. 383, 2022.
- [11] Xue Chen, Yueze Zheng, Junhuan Peng, and Mario Floris, "Monitoring river water level using multiple bounces of bridges in SAR images," *Advances in Space Research*, vol. 68, no. 10, 2021.
- [12] S. W. Kim and Y. K. Lee, "Accurate Water Level Measurement in the Bridge Using X-Band SAR," *IEEE Geoscience and Remote Sensing Letters*, vol. 19, 2022.
- [13] Ramon F. Hanssen, *Radar Interferometry: Data Inter*pretation and Error Analysis, Kluwer Academic Publisher, Dordrecht, 2001.
- [14] Geun Won Yoon, Sang Wan Kim, Yong Woong Lee, and Joong Sun Won, "Measurement of the water level in reservoirs from TerraSAR-X SAR interferometry and amplitude images," *Remote Sensing Letters*, vol. 4, no. 5, 2013.
- [15] Yoon Kyung Lee, Sang Hoon Hong, and Sang Wan Kim, "Monitoring of water level change in a dam from high-resolution sar data," *Remote Sensing*, vol. 13, no. 18, 2021.

- [16] Hannah Vickers, Eirik Malnes, and Kjell Arild Høgda, "Long-term water surface area monitoring and derived water level using synthetic aperture radar (SAR) at Altevatn, a medium-sized arctic lake," *Remote Sensing*, vol. 11, no. 23, 2019.
- [17] AHN, "Actueel Hoogtebestand Nederland (AHN)," 2019.
- [18] Bert M. Kampes, Radar Interferometry: Persistent Scatterer Technique, vol. 12, Springer Netherlands, Dordrecht, 2006.
- [19] Freek Van Leijen, *Persistent Scatterer Interferometry based on geodetic estimation theory*, Ph.D. thesis, Delft University of Technology, 2014.
- [20] Ke Wang and Jingyi Chen, "Accurate Persistent Scatterer Identification Based on Phase Similarity of Radar Pixels," *IEEE Transactions on Geoscience and Remote Sensing*, vol. 60, 2022.
- [21] Andrew Hooper, Howard Zebker, Paul Segall, and Bert Kampes, "A new method for measuring deformation on volcanoes and other natural terrains using InSAR persistent scatterers," *Geophysical Research Letters*, vol. 31, no. 23, 2004.
- [22] Wietske S. Brouwer and Ramon F. Hanssen, "A Treatise on InSAR Geometry and 3-D Displacement Estimation," *IEEE Transactions on Geoscience and Remote Sensing*, vol. 61, 2023.